

# CLUSTERING IN NUCLEI FROM $N/Z=1$ TO $N/Z=2$ \*

Wilton N. Catford

Department of Physics  
University of Surrey  
Guildford GU2 5XH, UK

**Abstract:** The clustering of nucleons in nuclei is a widespread but elusive phenomenon for study. Here, we wish to highlight the variety of theoretical approaches, and demonstrate how they are mutually supportive and complementary. On the experimental side, we describe recent advances in the study of the classic cluster nucleus  $^{24}\text{Mg}$ . Also, recent studies of clustering in nuclei approaching the neutron drip line are described. In the region near  $N/Z=2$ , both theory and experiment now suggest that multi-centre cluster structure is important, in particular for the very neutron rich beryllium isotopes.

## 1 INTRODUCTION: TYPES OF CLUSTERING

Rarely has a topic in nuclear physics attracted as much misunderstanding and debate as clustering behaviour in nuclei. Nuclear clusters are like Schrödinger's cats, being both in and out of existence until they are observed, and in some

\* Invited talk presented at "New Physics 2000" conference **The Nucleus: New Physics for the New Millenium** National Accelerator Centre, Faure, Cape Town, South Africa 18–22 January 1999 in *The Nucleus: New Physics for the New Millenium*, Proc. Int. Conf. held at Faure, Cape Town, January 1999, ed. F.D. Smit, R. Lindsay and S.V. Förtsch, ISBN 0-306-46302-4, (Kluwer Academic/Plenum, New York, 1999)

ways it is even more difficult to untangle their true behaviour from the process of observation. In some instances, such as the spectroscopic factors derived from  $\alpha$ -particle transfer reactions, the quantitative data give a sure signature of clustering [1]. More often, the signature is less definite but the cluster model leads to a consistent and intuitive understanding of the data. Taken as a whole, the evidence is compelling that clustering effects are important in nuclei across the periodic table, and particularly amongst the lighter nuclei below calcium. The richness of the subject has ensured a steady flow of recent review articles [2, 3, 4, 5].

The existence of  $\alpha$ -particle emission from nuclei suggests that pre-formed  $\alpha$ -particles might exist inside them. From very early on, however, it has been known [6, 7] that it is overly naive to suppose that any nucleus is composed of real  $\alpha$ -particles bound together. In a nucleus such as  $^{16}\text{O}$ , say, the  $\alpha$ -particles would overlap and effectively tear each other apart through the strong interaction. Still, as we shall see, the tendency towards clustering persists and it is driven by the tight binding of the maximally symmetric system of 2 protons and 2 neutrons coupled to  $L=S=0$ ; the  $(0s_{1/2})^4$  shell model configuration. The Ikeda diagram [8] predicts widespread clustering structure, and in particular  $\alpha$ -cluster structure, for states in nuclei at energies near the various cluster separation thresholds.

If we take  $^{12}\text{C}$  as an example, it is appealing to imagine three interacting  $\alpha$ -clusters dragging past each other in orbital motion, and exchanging nucleons through their strong interaction. For a given nucleon, its wavefunction is not confined to a single  $\alpha$ -cluster but is shared between different clusters. Perhaps it is reasonable to think of this as a kind of Bose-Einstein condensate of  $\alpha$ -particles. The overall A-body wavefunction must be antisymmetric, and it is the action of the antisymmetrization operator that effectively shares the wavefunction of each nucleon between the cluster mass centres. The average particle density distribution for the properly antisymmetrized intrinsic wavefunction of the nucleus continues to show the cluster-like appearance.

In some theoretical calculations, it is convenient to assume the existence of cluster centres *a priori*, and subsequently to deal with the antisymmetrization either exactly or according to an approximate prescription. Of course, the clusters need not in general be simply  $\alpha$ -like. Further, models have recently been developed that allow the general unconstrained A-body problem to be solved using a variational method, wherein the individual nucleons are allowed to move independently with a two-body force acting between them and are not forced into clusters at all. The results of such calculations show a natural tendency towards clustering behaviour in certain cases and mean field behaviour in others. One exciting prediction is that the light neutron rich nuclei such as beryllium, boron and carbon exhibit multicentre cluster structure as neutrons are added out towards the drip-line. This clustering may be a significant factor in determining the structure of neutron haloes in nuclei such as  $^{11}\text{Be}$  and  $^{14}\text{Be}$ . In any case, the models of halo nuclei which assume a core plus one or two

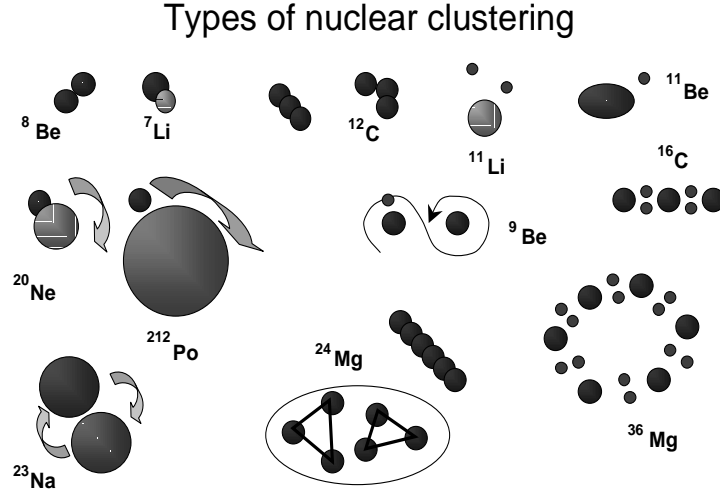
valence nucleons are examples of cluster models, where the core is treated as a cluster.

Clustering behaviour has been seen in a wide variety of guises [9, 10] across the nuclear chart, cf. fig.1, including:

- **Very light nuclei:** in cases such as  $^8\text{Be}$  ( $\alpha + \alpha$ ) [11] and  $^7\text{Li}$  ( $\alpha + t$ ) [12], or even  $^{12}\text{C}$  ( $3\alpha$ ) [13], there are small subsystems of the nucleus that are quite tightly bound and there is a tendency for this structure to develop and to be competitive in energy with a mean field configuration. Additional neutrons can be added into molecular orbitals in  $^8\text{Be}$  using the model of Abe [14] or otherwise and account for the properties of  $^9\text{Be}$  and  $^{10}\text{Be}$  [15, 16],
- **Magic core plus orbiting cluster:** in nuclei just beyond strong shell closures, the valence nucleons can behave like a cluster orbiting outside of the closed shell nucleus, giving characteristic rotational spectra, which have been observed near the  $^{16}\text{O}$ ,  $^{40}\text{Ca}$ ,  $^{90}\text{Zn}$  and  $^{208}\text{Pb}$  doubly magic closures [17]; this is discussed in the next section,
- **Normal core plus nucleon halo:** when for example the final neutron is extremely weakly bound within the mean field of the nucleus, then its wavefunction naturally tends to extend substantially beyond the edges of the nuclear potential into the classically forbidden region, particularly if it has a low angular momentum [18]; an even more interesting case is with two nucleons in the halo, such as in Borromean systems [19],
- **Large-scale clustering in low-lying levels:** complex nuclei have been successfully modelled with the assumption that they comprise two mutually orbiting nuclei of comparable masses, with the predicted spectra showing remarkable agreement from the ground state all the way up to the separation energy [20, 21, 22]; this, despite the fact that the components must surely overlap,
- **Large-scale clustering at high excitation:** resonances seen at energies near the Coulomb barrier in heavy ion scattering [23, 24, 25], particularly between  $\alpha$ -conjugate nuclei, seem to indicate molecular-like states in which the component nuclei orbit at a distance where they just graze against each other [25, 26]; this can also be studied in breakup reactions,
- **Complete alpha-particle condensation:** an extreme form of clustering behaviour is predicted in some models for  $A = 4n$  nuclei, wherein the entire nucleus behaves not as one liquid drop but as a condensation into  $n$  separate  $\alpha$ -like droplets [13, 27], and when extra excitation energy is added to these nuclei the configuration of the mass centres can unwrap and become spatially extended; the limiting case is represented by linear chain states, which have been predicted over a wide range of masses [28].

The various different models that have been developed are described in the reviews [2, 3, 4, 5]. One theoretical approach is to treat the clusters within

**Figure 1** A wide variety of different types of clustering behaviour have been identified in nuclei, from small clusters outside of a closed shell, to complete condensation into  $\alpha$ -particles, to halo nucleons outside of a normal core.



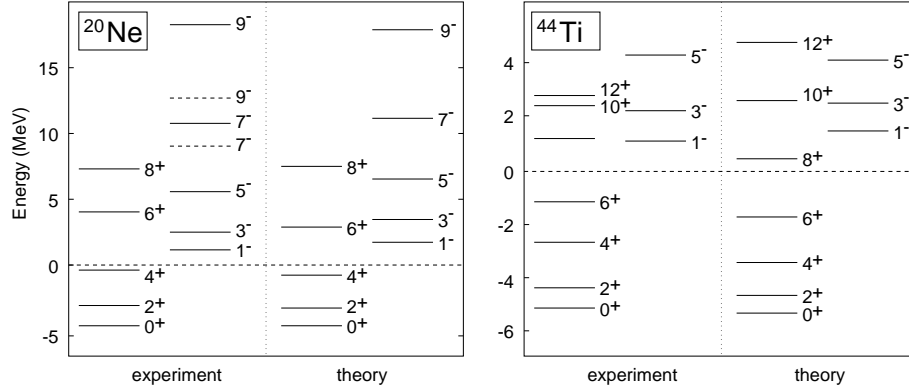
the nucleus as real clusters and to solve the many-body scattering problem, for example in the three-body case by solving the three-body Faddeev equations [19]. This can be successful provided that the clusters avoid overlapping. Alternatively, the cluster structure can be assumed but the exchange of nucleons can be allowed, and the wavefunctions properly antisymmetrized. Such models using the resonating group method (RGM) [5, 29] and the generator coordinate method (GCM) [30] have been extensively applied to light nuclei and in particular for calculations of astrophysically important processes. Group theoretic approaches have been used to analyse the symmetry properties of cluster states [31]. Approximate two-body models have been applied to nuclei where a cluster orbits a core [32], with the orbital quantum numbers chosen in such a way as to approximately satisfy the Exclusion Principle by avoiding the overlap of the core and cluster wavefunctions. Another model that has been widely applied is the Brink-Bloch  $\alpha$ -cluster model [13, 27], in which nucleons are assumed to be bound in harmonic potential wells forming  $\alpha$ -like clusters with  $L=S=0$ . An effective two-body force acts between the clusters and a fully antisymmetrized A-body Slater determinant wavefunction is derived. The equilibrium positions of the mass centres are determined in a variational calculation. Time dependence can be introduced to this model to give the time-dependent cluster model (TDCM) [33]. Taking this one step further, individual unconstrained nucleons can be treated in a similar fashion with a two-body force acting between independently moving nucleons. This approach has been developed into models

known as Fermionic molecular dynamics [34] and antisymmetrized molecular dynamics (AMD) [35]. The quantities that can be calculated in the various models vary from case to case, but energy levels, electromagnetic moments and transition densities have all been very successfully predicted. An exciting recent development in theory, via the AMD model, is the ability to predict systematically the persistence of clustering in systems that differ from the simple  $A = 4n, T_z = 0$   $\alpha$ -like nuclei, and this will be discussed below.

## 2 REVIEW OF SOME KEY RESULTS FROM THE MODELS

### 2.1 Positive and negative parity rotational bands

**Figure 2** The energy offset between positive and negative parity states in rotational bands, shown here for the ground state bands in  $^{20}\text{Ne}$  and  $^{44}\text{Ti}$ , supports the cluster model.



In  $^{20}\text{Ne}$  for example, there is a negative parity  $K=0$  rotational band with the same moment of inertia as the positive parity ground state band, but displaced upwards in energy. The natural explanation for this in terms of the cluster model was first put forward by Horiuchi and Ikeda [36]. These bands correspond to an  $\alpha$ -particle orbiting an  $^{16}\text{O}$  core [37]. Assuming that it is possible to start with an  $\alpha$ -particle on one side of the core and to pass continuously, via the radial motion of the cluster, to the situation with it on the opposite side of the core, then this implies a symmetric potential energy function that has a barrier at zero separation. The intrinsic solutions centred on the two minima must be properly symmetrized to obtain states of good parity, and the resultant states of different parity have different behaviour in the region of the central barrier. The negative parity state vanishes at zero but the positive parity state does not. The net effect is to shift negative parity states upwards in energy compared to the positive parity states. This behaviour is clearly seen in  $^{20}\text{Ne}$  and also in  $^{44}\text{Ti}$ , where an  $\alpha$ -particle orbits a  $^{40}\text{Ca}$  core (see fig. 2, [38]). In fact, if the barrier between the two reflection symmetric states (before parity projection) became infinitely large, then the probability of being at zero

would be zero for the positive parity solution also, and there would be no shift between the different parity rotational states in that case. This closely parallels the situation for octupole deformation in nuclei, where intrinsic octupole states can be continuously transformed into their degenerate mirror images. In their review of intrinsic reflection asymmetry, Butler and Nazarewicz [39] point out that the *sd*-shell region provided the first evidence for reflection asymmetry in rotating nuclei, and they include a detailed bibliography for studies of  $^{16}\text{O}$ ,  $^{18}\text{O}$ ,  $^{20}\text{Ne}$ ,  $^{24}\text{Mg}$ ,  $^{28}\text{Si}$ ,  $^{32}\text{S}$ ,  $^{40}\text{Ca}$  and  $^{44}\text{Ti}$ , concentrating on the octupole aspects.

Another important point to note is that the level scheme of *core + cluster* nuclei is not the only property which is well reproduced by cluster model calculations. Using models such as that of Buck, Dover and Vary [32], electromagnetic transition densities can be calculated correctly, without the need for effective charges such as required in shell model calculations. These calculations have been extended successfully to include  $\alpha$ -particle states above the  $^{90}\text{Zr}$  and  $^{208}\text{Pb}$  double shell closures [17]. Alpha-decay widths and low energy elastic scattering cross sections have been reproduced in a unified treatment for  $^{20}\text{Ne}$  and  $^{44}\text{Ti}$  [38]. The model can be extended successfully to nuclei in which exotic clusters (those which have been observed in radioactivity, such as  $^{24}\text{Ne}$  [40]) orbit outside of a  $^{208}\text{Pb}$  core. Buck *et al* successfully reproduced the systematics of exotic decay half-lives [41] and also the excitation energies for rotational bands (including Coriolis antistretching) and electromagnetic transition strengths for collective quadrupole and octupole transitions [42] across 19 even-even actinide nuclei.

## 2.2 The structure of $^{12}\text{C}$

The nucleus  $^{12}\text{C}$  has long been treated theoretically as a triangular arrangement of  $\alpha$ -like structures [13]. Models that presuppose the existence of clusters, such as that of Brink [13], have recently received extra theoretical support from two different directions. In the first instance, the quantum mechanical three-body problem, including the Coulomb force, was solved for real  $\alpha$ -particles using a hyperspherical expansion of the Faddeev equations [43]. A phenomenological three-body force was included to account for Pauli and polarization effects. With parameters chosen to reproduce the energy of the three-body ( $0_2^+$ , 7.65 MeV) scattering state, the width of the  $0_2^+$  and the energy of the bound  $0_1^+$  ground state were reasonably reproduced. The calculations predicted the most likely relative spatial configurations of the three  $\alpha$ -particles in the scattering problem. The ground state was an almost pure equilateral triangle with sides of 3.0 fm, whereas the excited (unbound) state was a superposition of several configurations with the main one being a somewhat larger and flattened triangle. The ground state result is quite close to the geometry found in a GCM calculation which used an equilateral triangle with the length of the sides being a fitted parameter [44]. The ( $0_2^+$ , 7.65 MeV) state was once thought [45] to be an example of a linear  $\alpha$ -particle chain state of the type postulated by Morinaga [46]. Later work showed that the  $0_2^+ - 2_2^+$  energy gap was not consistent with a linear  $3\alpha$  linear chain structure [47] and a bent chain

was proposed [48]. The three-body Fadeev calculations support this general interpretation although they imply a hinge angle of around  $100^\circ$  in the dominant configuration rather than the  $150^\circ$  favoured by earlier calculations [49].

Another recent theoretical treatment of  $^{12}\text{C}$  is that of Kanada-En'yo [50]. She used the antisymmetrized molecular dynamics (AMD) model [2, 35], extended to perform the variational part of the calculation after projecting states of good parity and angular momentum. In these calculations, the relative geometry of the individual nucleons was not constrained at all *a priori*, i.e no clustering was imposed on the nucleus. The predicted spectrum of levels and their transition strengths show several advantages over cluster calculations, in particular for the relative properties of the  $0_1^+$  ground state and the  $0_2^+$  state. An analysis of the wavefunctions obtained [50] shows that the  $\alpha$ -clusters are significantly dissociated in the ground state, but the results also support a well-developed  $3\alpha$  structure for other rotational bands.

### 2.3 Dissolution of alpha particles

As discussed above,  $^{20}\text{Ne}$  displays a rotational band spectrum that indicates an  $^{16}\text{O}+\alpha$  structure. Recently, within the framework of the AMD model, it has become possible to study theoretically the degree of clustering in the different states of the band [35]. These new calculations support many of the earlier deductions [51] concerning reduced clustering in the ground state band towards its termination at spin  $8^+$ . A cranking method was used to study states along the yrast line in  $^{20}\text{Ne}$ , starting from the overall minimum energy solution for the  $0^+$  ground state. Nucleon density distributions were then calculated for the rotating intrinsic states before parity projection. For the lower states in the band, the structure was found to be prolate and approximately axially symmetric, consistent with an  $^{16}\text{O}+\alpha$  structure. Furthermore, the  $^{16}\text{O}$  part of the mass density comprised a tetrahedral arrangement of four  $\alpha$ -like mass centres arranged as predicted by conventional cluster models of  $^{16}\text{O}$ . The negative parity states showed particularly well-developed clustering. For spins of  $7^-$  and above, the  $^{16}\text{O}+\alpha$  structure tended to dissolve and other structures including oblate shapes and  $^{12}\text{C}\alpha\alpha$  cluster configurations began to appear. Although they have certain deficiencies, for example the negative parity energies are not well reproduced, the calculations give a fascinating insight into the evolution of clustering with excitation energy and spin. At the higher excitation energies they help to delineate the limits of applicability for cluster models. At the lower energies the AMD results strongly support the validity of assuming a cluster structure, and hence they support the predictions of other quantities that can be made most effectively using the cluster models.

### 2.4 Large-scale or di-nuclear clustering

Calculations using an  $\alpha$ -cluster model for a large nucleus sometimes give solutions that show a tendency for the nucleus to be grouped into two or more substantial substructures. This generalises the behaviour seen for  $^{20}\text{Ne}$  in the

AMD. Indeed, the calculations of Marsh and Rae [52] using the Brink model [13] show that the ground state of  $^{24}\text{Mg}$  can be viewed as two  $^{12}\text{C}$  nuclei in juxtaposition. In a certain sense, therefore, it is not too surprising that the low-lying levels of nuclei such as  $^{24}\text{Mg}$  can be modelled as two interacting  $^{12}\text{C}$  nuclei. What is truly remarkable, however, is that such a model [21, 22] succeeds with the component nuclei taking on their free-space properties, even though they presumably overlap considerably.

In the approach of Buck *et al* [21],  $^{24}\text{Mg}$  is modelled as a bound state of two  $^{12}\text{C}$  nuclei which can be internally excited. The internal energy levels and the electromagnetic transition strengths between them are taken to be those for real, free  $^{12}\text{C}$  nuclei. Coupled channels calculations are performed to deduce the level scheme up to a maximum energy given by the sum of the Coulomb barrier and the  $^{12}\text{C}+^{12}\text{C}$  separation energy. Almost the entire experimentally known  $T=0$  spectrum is reproduced, both for positive and negative parity states. The calculated electromagnetic strengths for quadrupole transitions between the low-lying positive parity states are also in good agreement with experimental values, without the need to introduce effective charges. The model has been extended to describe  $^{23}\text{Na}$  in terms of  $^{12}\text{C}$  and  $^{11}\text{B}$ , each with their free-space properties [20]. Excellent agreement is achieved with experimental E2 and M1 transition strengths, and the model has also been extended successfully to predict polarization observables [53]. Whether such models have a physical significance beyond their computational convenience is not clear.

### 2.5 Natural clustering tendency in neutron rich systems

When additional neutrons are added to the  $^8\text{Be}$  core of two  $\alpha$ -clusters, molecular states in  $^9\text{Be}$  and  $^{10}\text{Be}$  are formed [15, 16, 54]. Similarly, protons can be added and account for structures in the nuclei  $^9\text{B}$  and  $^{10}\text{B}$  [16, 55]. These approaches can be extended to the more neutron rich isotopes of beryllium and boron [15, 56, 57] and to analogous  $3\alpha$  systems in the carbon isotopes [56]. Thus, Nature edges towards the speculative suggestion of Wilkinson [58] that complete rings of  $\alpha$ -clusters might exist, like necklaces, held together by neutron pairs in covalent bonds between the clusters (cf. fig.1). For now, however, necklace states remain pure speculation and even simple chain states of  $\alpha$ -clusters (which are predicted to exist at high excitations over a range of nuclei [28]) are not compellingly in evidence experimentally beyond  $^8\text{Be}$ .

Von Oertzen [16, 56] has estimated the excitation energies of molecular chain states in neutron rich beryllium, boron, carbon and oxygen, where the  $\alpha$ -cluster centres are bound together with covalent bonds in analogy with the well-known [15, 54]  $\alpha:2n:\alpha$  states near 6 MeV in  $^{10}\text{Be}$ . The chain states are expected to be at higher excitation energies in the more exotic nuclei [16, 56], although other clustering (e.g.  $^{12}\text{Be}=^6\text{He}+^6\text{He}$ ) could be anticipated at lower excitations.

But what of the wider significance of clustering in the lowest energy levels for light, neutron rich nuclei? An exciting development in the study of these nuclei has been the AMD predictions for ground state nucleon densities. Calculations have been performed for isotopic chains extending to the neutron dripline for



ground states of lithium and beryllium [59, 60], boron [61] and carbon [62, 63] and have been summarised by Horiuchi [2]. As might be expected, a tendency towards clustering is predicted near the  $N=Z$  line and a tendency towards more mean-field behaviour near the magic number  $N=8$ . However, for  $N>8$  the clustering appears to return and in some cases to be enhanced. For example, in boron isotopes the proton intrinsic matter distributions show marked and increasing Li-He clustering in the isotopes  $^{15,17,19}\text{B}$ . Across isotopic chains, the AMD calculations have been tested against measured ground state properties and they are found to reproduce well the radii, binding energies and magnetic moments, except in the case of known halo states [2]. Similarly, the excited state energy spectra and the electromagnetic transition strengths between levels are reproduced quite well, except for halo levels.

The structure of excited states, and the evolution of shape within a given nucleus have been studied in more detail in very recent work with the AMD model for  $^{10}\text{Be}$  [64] and  $^{12}\text{C}$  [50]. The AMD calculations highlight very clearly the differences in structure, for example between the ground state of  $^{10}\text{Be}$  and the quartet of molecular states near 6 MeV [64]. They allow the coexistence of cluster structure and mean field structure to be investigated. Otherwise, in the explicitly molecular models [56, 57] the relationship between the lowest states and the excited molecular states requires careful interpretation.

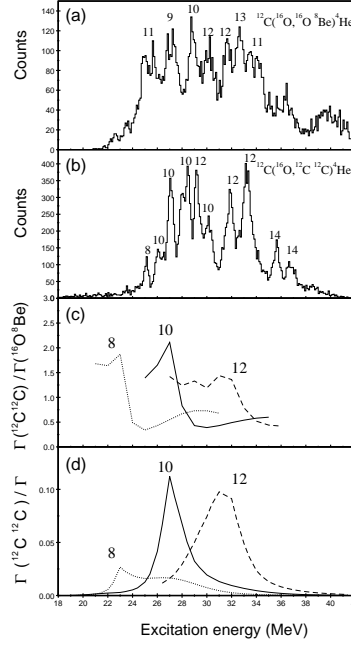
### 3 RECENT EXPERIMENTAL RESULTS

#### 3.1 Breakup of $^{24}\text{Mg}$ to $^{12}\text{C}+^{12}\text{C}$

The breakup of excited  $^{24}\text{Mg}$ ,  $^{28}\text{Si}$  and  $^{32}\text{S}$  nuclei into  $^{12}\text{C}$  and  $^{16}\text{O}$  fragments, following nuclear excitation processes, has been studied in detail for more than a decade [3]. The widths of the  $^{24}\text{Mg}$  breakup states are of order 100–150 keV [65] which is comparable to the expected statistical width [66]. On the other hand the breakup states and the resonances populated in  $^{12}\text{C} + ^{12}\text{C}$  scattering near the barrier appear to be closely linked [65], and the scattering resonances have been shown to have enhanced partial widths for  $^{12}\text{C}$  decay. The scattering resonances are also correlated between different reaction channels and they  $\gamma$ -decay to the ground state of  $^{24}\text{Mg}$  [24].

For the breakup states, there has never been a direct partial width measurement. Recently, Freer *et al.* have attempted to obtain such information indirectly, by comparing the probabilities for the decay of  $^{24}\text{Mg}$  states into the  $^{12}\text{C}+^{12}\text{C}$  and  $^{16}\text{O}+^8\text{Be}$  channels [67]. States in  $^{24}\text{Mg}$  were populated in the reaction  $^{12}\text{C}(^{16}\text{O},\alpha)^{24}\text{Mg}$  at several beam energies and the spins were measured using the angular correlations of the sequential breakup. The energy-spin systematics followed the grazing angular momentum for two  $^{12}\text{C}$  nuclei (as expected for molecular states). However, it was also noted that the statistical decay probabilities for fission to two ground state  $^{12}\text{C}$  nuclei follow similar systematics, peaking as the barrier penetration probabilities balance against the opening of competing channels (cf. Fig.3). In a quantitative analysis, it appeared that some states decayed to the two fission channels with the statis-

**Figure 3** Montage of excitation spectra for breakup states seen in  $^{24}\text{Mg}$  depopulated by (a)  $^{16}\text{O}^8\text{Be}$  or (b)  $^{12}\text{C}^{12}\text{C}$  decay. Also shown, statistical partial width predictions as a function of excitation energy and spin, for (c)  $^{12}\text{C}^{12}\text{C}$  relative to  $^{16}\text{O}^8\text{Be}$  and (d) for  $^{12}\text{C}^{12}\text{C}$  as a fraction of the total width.

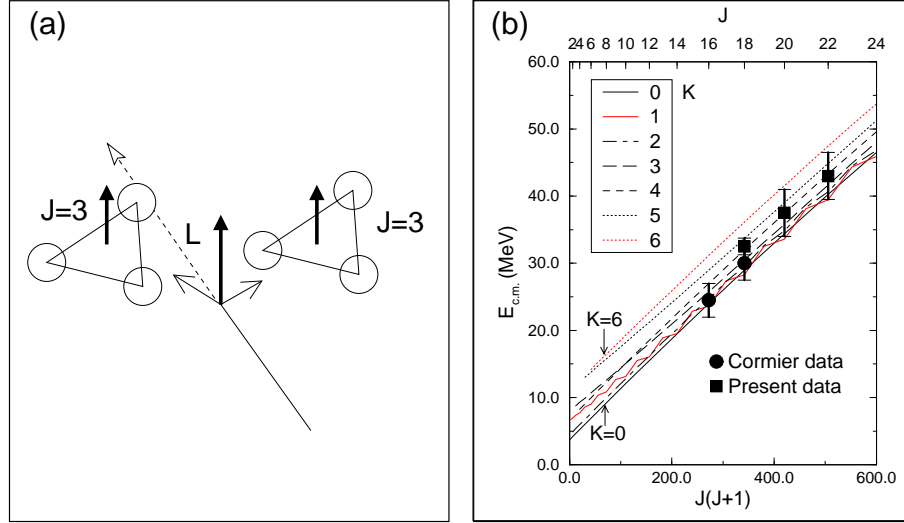


tical ratio of probabilities, but that in addition there were several states that favoured the  $^{12}\text{C}+^{12}\text{C}$  channel. The situation may have been particularly complicated because the breakup states were populated using the  $(^{16}\text{O},\alpha)$  reaction, which has a compound nuclear mechanism according to its angular distribution [68]. The mechanism in  $^{12}\text{C}(^{24}\text{Mg}, ^{24}\text{Mg}^*)^{12}\text{C}$  or in transfer reactions may be more selective of true molecular states. Clearly, there is a lot more work still to be done in the measurement of partial decay widths for breakup states.

### 3.2 Resonances in mutual $3^-$ scattering of $^{12}\text{C}+^{12}\text{C}$

Chappell *et al.* [71] have recently measured excitation functions and angular correlations for  $^{12}\text{C}+^{12}\text{C}$  scattering leading to mutual excitation of the  $^{12}\text{C}^*(9.63\text{ MeV}; 3_1^-)$  state. In the Brink-Bloch model, both the ground state and the  $3_1^-$  state have the same intrinsic triangular shape, and the  $3_1^-$  state has three units of angular momentum around its three-fold symmetry axis. The new mutual  $3_1^-$  data complement earlier measurements of the mutual  $0_2^+$  (7.65

**Figure 4** Resonances seen in  $^{12}\text{C}+^{12}\text{C}$  scattering to the mutual  $3_1^-$  channel: (a) the angular correlations indicate fully aligned angular momentum in the final state as shown schematically, (b) the energy-spin systematics are consistent with  $\alpha$ -cluster predictions for a very deformed triaxial state in  $^{24}\text{Mg}$ .



MeV) channel [72] and the  $0_2^+3_1^-$  channel [73, 74] and extend over the energy range  $E_{\text{cm}} = 30\text{--}45$  MeV.

The  $3_1^-$  state decays by  $\alpha$ -emission to produce a jet of three  $\alpha$ -particles, and these must be reconstructed kinematically in the analysis to flag  $3_1^-$  production. In fact, the experiment needed to measure five-fold coincidences and reconstruct the sixth  $\alpha$ -particle prior to the reconstructions of the triple jets. In the excitation function, prominent resonances were observed at  $E_{\text{cm}} = 32.5$ , 37.5 and 43.0 MeV. The lowest of these corresponds to the energy of the famous resonance in  $0_2^+0_2^+$  scattering [72] that was once believed to correspond to a shape eigenstate resonance in the form of a  $6\alpha$  linear chain [75], but the  $3_1^-3_1^-$  channel is found to be much stronger [73]. In view of the triangular structure of the  $3_1^-$  state, the  $6\alpha$  chain hypothesis is untenable. It can be supposed that the strength in the  $0_2^+0_2^+$  channel arises through the hinge angle in the  $3\alpha$   $0_2^+$  state (see earlier), which gives it a partially triangular structure.

The angular correlation analysis for the  $3_1^-3_1^-$  scattering reveals that the final state is fully aligned in angular momentum, as shown schematically in fig. 4(a). The dominant spins for the three resonances appear to be 18, 20 and 22 respectively. These high spins cannot be supported by  $^{24}\text{Mg}$  in its normal deformation [71], so the absorptive scattering potential is in principal weaker (since only direct reactions and highly deformed resonances contribute).

Chappell *et al.* discuss their results in the context of the Band Crossing Model [76] using reaction theory, and they use the Brink-Bloch  $\alpha$ -cluster model to give a structural interpretation. The Brink model predicts [52] a strongly deformed triaxial state with  $^{12}\text{C}^{12}\text{C}$  structure, which corresponds to that labelled F1 by Flocard *et al.* [77]. When this rotates, it gives rise to a number of bands with different K-values which are close in energy but have very little K-mixing. It was speculated [71] that the  $3_1^- 3_1^-$  resonances (see fig. 4(b)) may be associated with the K=6 component, and that they extend the sequence of broad resonances first observed by Cormier *et al.* [78] in single and mutual  $2_1^+$  scattering.

### 3.3 Search for gamma-ray decay of breakup states in $^{24}\text{Mg}$

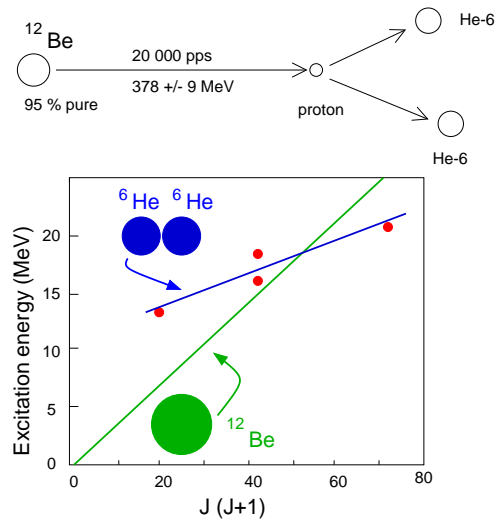
The  $^{12}\text{C}+^{12}\text{C}$  states seen in breakup and resonance reactions appear to show rotational  $J(J+1)$  systematics. This could be a genuine structural effect or it could be due to some kinematic selection. To distinguish these possibilities, the observation of decay  $\gamma$ -rays connecting the states would be useful, but this is exceptionally difficult. One experiment has so far succeeded in obtaining results [69]. A well known  $10^+$  resonance at  $E_{\text{cm}} = 16.45$  MeV was populated in  $^{12}\text{C}+^{12}\text{C}$  scattering. Particles were detected in coincidence using two position sensitive detectors to record their energy and angle. The complete binary kinematics allowed the masses of the particles in the exit channel to be determined, and the  $^{12}\text{C}+^{12}\text{C}$  channel could be selected. An array of 74 BaF<sub>2</sub> detectors (Château de Cristal) recorded coincident  $\gamma$ -rays. The reaction Q-value was reconstructed and the missing kinetic energy was compared with the  $\gamma$ -ray energy. If the resonance  $\gamma$ -decayed to a lower state in  $^{24}\text{Mg}$ , that subsequently decayed to  $^{12}\text{C}_{\text{gs}}+^{12}\text{C}_{\text{gs}}$ , then the compared energies should be equal. The principal complication and source of background comes from events in which the breakup precedes the  $\gamma$ -decay, that is when the resonance decays to one (or even two) excited  $^{12}\text{C}$  fragments. This is dominated by the 4.43 MeV,  $2_1^+$  channel. No simple discrimination of these events, other than by  $\gamma$ -ray energy, can be made. The result from the experiment was quoted as  $\Gamma_\gamma/\Gamma = 1.2 \times 10^{-5}$  which, with certain assumptions, corresponds to a transition strength of order 100 W.u. These numbers are comparable to the predictions for a molecular band [69, 70], but because of the low statistics and the background uncertainties it seems most appropriate to interpret them as upper limits. More experiments are definitely required.

### 3.4 Two-centre effects in neutron-rich Be isotopes

The beryllium isotopes, as discussed above, are predicted to exhibit a well developed molecular structure in which valence neutrons bind together two helium-like centres [56, 64]. The molecular states are expected near the threshold for  $^4\text{He}$  and  $^6\text{He}$  decay, consistent with the Ikeda diagram [8]. Recently, experimental evidence in support of these predictions has been obtained in a measurement of  $p(^{12}\text{Be}, ^{12}\text{Be}^*)p$  using a radioactive beam [79]. A beam of 378

MeV  $^{12}\text{Be}$  ions was produced at the GANIL laboratory using the LISE3 spectrometer. The fragmentation products from a primary  $^{18}\text{O}$  beam were purified to produce a beam of 95%  $^{12}\text{Be}$  at  $2 \times 10^4$  pps. Fragments from the binary breakup of  $^{12}\text{Be}^*$  were identified by Z and A in E. $\Delta$ E telescopes. Measurements of the angles and energies allowed the excitation energy of the parent  $^{12}\text{Be}$  to be reconstructed. Evidence was obtained for both  $^6\text{He}^6\text{He}$  and  $\alpha^8\text{He}$  breakup, beginning at an excitation energy just above threshold (close to 10 MeV in each case). The  $^6\text{He}^6\text{He}$  spectrum is less complicated because the identical spin zero particles restrict the states to even spin and parity. Unfortunately, no partial width measurements were possible. Remarkably, the relative angular distributions of the  $^6\text{He}^6\text{He}$  breakup fragments could be measured sufficiently accurately to suggest spin assignments for several levels. The result was an approximate rotational sequence (fig. 5, [79]) reminiscent of the results for  $^{12}\text{C}^{12}\text{C}$  breakup of  $^{24}\text{Mg}$  [80]. The moment of inertia is consistent with two touching  $^6\text{He}$  spheres and greatly exceeds that for a spherical  $^{12}\text{Be}$  nucleus. Now that there is experimental evidence to support the theoretical suggestions of clustering in the neutron rich beryllium isotopes, it is likely that clustering and two-centre effects must be taken into account in all studies of this region. This is relevant in view of the recent measurements of  $p(^{11}\text{Be}, ^{10}\text{Be})d$  spectroscopic factors with a radioactive beam [81], which represent the beginning of transfer reaction spectroscopy far from stability.

**Figure 5** Inelastic scattering of a radioactive beam of  $^{12}\text{Be}$  has shown breakup of  $^{12}\text{Be}$  into  $^6\text{He}^6\text{He}$ , and the spins of the breakup states are consistent with a rotational band for two touching  $^6\text{He}$  spheres. The steeper trajectory for a spherical  $^{12}\text{Be}$  is shown for comparison.



## 4 OUTLOOK

Nuclear level schemes reveal an underlying cluster structure in many circumstances. One of the most intriguing continues to be the large-scale structure epitomised by  $^{24}\text{Mg}$  as  $^{12}\text{C}+^{12}\text{C}$ . Evidence exists that some excited states in  $^{24}\text{Mg}$  have a preference (beyond the statistical probability) for decay into two  $^{12}\text{C}$  fragments, but the interpretations are open to ambiguities. A key requirement is for partial decay widths such as  $\Gamma(^{12}\text{C})/\Gamma$  to be measured for breakup states. The recent experiments using  $^{12}\text{C}(^{16}\text{O}, ^{12}\text{C}^{12}\text{C})\alpha$  and  $^{12}\text{C}(^{12}\text{C}, ^{12}\text{C}\gamma)^{12}\text{C}$  give some indication of how this might be done. Meanwhile, as experimental techniques advance,  $^{12}\text{C}+^{12}\text{C}$  scattering continues to show remarkable behaviour such as the fully aligned angular momentum in mutual  $3_1^-$  scattering. The recent  $3_1^-3_1^-$  experiment probed  $^{24}\text{Mg}$  at high spins, beyond the normal fission limit, in a regime where less ambiguities may exist owing to the lower level density.

Probably the most exciting prospects in cluster studies are amongst the light, very neutron rich nuclei. The AMD calculations have finally taken clustering away from magic shells and the  $N=Z$  line, and away from cluster models themselves. The importance of clustering up until now has largely been in the computational power that it provides when the clustering symmetry in the structure is recognised in the formulation of the model. What is somewhat different about the AMD work is that it implies, with no *a priori* assumptions, that it is necessary to take clustering into account in order to get any proper understanding of the structure of light neutron rich nuclei, even in their ground states. The recent results for the  $^6\text{He}^6\text{He}$  breakup of  $^{12}\text{Be}$  point the way to many exciting experiments in the future, using radioactive beams to explore this region far from stability in a way that was not possible with stable beams.

## Acknowledgments

The work described here derives from the author's work over a number of years with the CHARISSA collaboration, and their support and contributions are gratefully acknowledged. Thanks also to Sharpey, for encouragement back in the thesis days.

## References

- [1] A. Arima and S. Kubono, *in* Treatise on Heavy-Ion Science, Vol. 1, ed. D.A. Bromley (Plenum, New York, 1984) p.617
- [2] H. Horiuchi, *in* Correlations and Clustering Phenomena in Subatomic Physics, ed. M. Harakeh *et al.*, Plenum Press (New York) 1997, pp.29-51
- [3] M. Freer and A.C. Merchant, J. Phys. **G23** (1997) 261
- [4] A.H. Wuosmaa *et al.*, Annu. Rev. Nucl. Part. Sci. **45** (1995) 89
- [5] K. Langanke, Adv. Nucl. Phys. **21** (1994) 85
- [6] J.A. Wheeler, Phys. Rev. **59** (1941) 16 and 27
- [7] W. Wefelmeier, Z. Phys. **107** (1937) 332; Naturwiss. **25** (1937) 525

- [8] K. Ikeda *et al.*, Prog. Th. Phys. Suppl. Extra Number (1968) 464
- [9] R.K. Sheline and K. Wildermuth, Nucl. Phys. **21** (1960) 196
- [10] J. Cseh and W. Scheid, J. Phys. **G18** (1992) 1419
- [11] J.A. Wheeler, Phys. Rev. **52** (1937) 1083,1107
- [12] B. Buck *et al.*, J. Phys. **G11** (1985) L11; **G14** (1988) L211
- [13] D.M. Brink, *in* Proc. Int. School of Physics “Enrico Fermi”, course XXXVI, Varenna, 1965, ed. C. Bloch (Academic Press, New York, 1966) p.247
- [14] Y. Abe, J. Hiura and H. Tanaka, Prog. Theor. Phys. **49** (1973) 800
- [15] M. Seya, M. Kohno and S. Nagata, Prog. Theor. Phys. **65** (1981) 205
- [16] W. von Oertzen, Z. Phys. **A357** (1997) 355
- [17] B. Buck, A.C. Merchant and S.M. Perez, Phys. Rev. **C51** (1995) 559
- [18] K. Riisager, Rev. Mod. Phys. **66** (1994) 1105
- [19] M.V. Zhukov *et al.*, Phys. Rep. **231** (1993) 151
- [20] A. Kabir and B. Buck, Nucl. Phys. **A518** (1990) 449
- [21] B. Buck, P.D.B. Hopkins, A.C. Merchant, Nucl. Phys. **A513** (1990) 75
- [22] R. Baldock, B. Buck and J.A. Rubio, J. Phys. **G12** (1986) L29
- [23] D.A. Bromley *et al.*, Phys. Rev. Lett. **4** (1960) 365 and 515
- [24] K.A. Erb and D.A. Bromley, *in* Treatise on Heavy-Ion Science, Vol. 3, ed. D.A. Bromley (Plenum, New York, 1985) p.201
- [25] N. Cindro, Riv. N. Cimento **4** (1981) No.6; Ann. Phys. Fr. **13** (1988) 289
- [26] H. Feshbach, Proc. European conf. on nuclear physics with heavy ions, Caen, France, 1976. J. de Physique (Colloque) **37** (1976) C5:177
- [27] W.D.M. Rae, Int. J. Mod. Phys. **A3** (1988) 1343
- [28] A.C. Merchant and W.D.M. Rae, Nucl. Phys. **A549** (1992) 431
- [29] K. Wildermuth and Y.C. Yang, A Unified Theory of the Nucleus, (Academic Press, New York, 1977)
- [30] P. Descouvemont *et al.*, Nucl. Phys. **A605** (1996) 160
- [31] J. Cseh and W. Scheid, J. Phys. **G18** (1992) 1419
- [32] B. Buck, C.B. Dover and J.P. Vary, Phys. Rev. **C11** (1975) 1803
- [33] W. Bauhoff *et al.*, Phys. Rev. **C32** (1985) 150
- [34] H. Feldmeier, Nucl. Phys. **A515** (1990) 147
- [35] Y. Kanada-En’yo and H. Horiuchi, Prog. Theor. Phys. **93** (1995) 115
- [36] H. Horiuchi and K. Ikeda, Prog. Theor. Phys. **40** (1968) 277
- [37] K. Wildermuth, T. Kenelopoulos, Nucl. Phys. **7** (1958) 150; **9** (1958) 449
- [38] B. Buck *et al.*, Phys. Rev. **C52** (1995) 1840
- [39] P.A. Butler and W. Nazarewicz, Rev. Mod. Phys. **68** (1996) 349
- [40] H.J. Rose and G.A. Jones, Nature **307** (1984) 245
- [41] B. Buck, A.C. Merchant and S.M. Perez, Phys. Rev. Lett. **76** (1996) 380

- [42] B. Buck, A.C. Merchant and S.M. Perez, Phys. Rev. **C58** (1998) 2049
- [43] D.V. Fedorov and A.S. Jensen, Phys. Lett. **B389** (1996) 631
- [44] M. Dufour and P. Descouvemont, Nucl. Phys. **A605** (1996) 160
- [45] H. Morinaga, Phys. Lett. **21** (1966) 78
- [46] H. Morinaga, Phys. Rev. **101** (1956) 254
- [47] Y. Fujiwara *et al.*, Prog. Th. Phys. Suppl. **68** (1980) 29
- [48] H. Horiuchi, K. Ikeda and Y. Suzuki, Prog. Th. Phys. Suppl. **52** (1972) 89
- [49] H. Friedrich, L. Satpathy and A. Weiguny, Phys. Lett. **B36** (1971) 189
- [50] Y. Kanada-En'yo, Phys. Rev. Lett. **81** (1998) 5291
- [51] A. Arima, H. Horiuchi, K. Kubodera and N. Takigawa, Adv. Nucl. Phys. **5** (1972) 345; T. Tomoda and A. Arima, Nucl. Phys. **A303** (1978) 217
- [52] S. Marsh and W.D.M. Rae, Phys. Lett. **B153** (1985) 21
- [53] A. Kabir and R.C. Johnson, J. Phys. **G18** (1992) 1967
- [54] S. Okabe and Y. Abe, Prog. Theor. Phys. **61** (1979) 1049
- [55] H. Furutani *et al.*, Prog. Theor. Phys. Suppl. **68** (1980) 193
- [56] W. von Oertzen, Z. Phys. **A354** (1996) 37
- [57] W. von Oertzen, Il Nuovo Cimento **110A** (1997) 895
- [58] D.H. Wilkinson, Nucl. Phys. **A452** (1986) 296
- [59] Y. Kanada-En'yo, H. Horiuchi and A. Ono, Phys. Rev. **C52** (1995) 628
- [60] A. Doté, H. Horiuchi and Y. Kanada-En'yo, Phys. Rev. **C56** (1997) 1844
- [61] Y. Kanada-En'yo and H. Horiuchi, Phys. Rev. **C52** (1995) 647
- [62] Y. Kanada-En'yo and H. Horiuchi, Phys. Rev. **C55** (1997) 2860
- [63] Y. Kanada-En'yo and H. Horiuchi, Phys. Rev. **C54** (1996) R468
- [64] Y. Kanada-En'yo, H. Horiuchi and A. Doté, J. Phys. **G24** (1998) 1499
- [65] N. Curtis *et al.*, Phys. Rev. **C51** (1995) 1554
- [66] D. Shapira, R.G. Stokstad and D.A. Bromley, Phys. Rev. **C10** (1974) 1063
- [67] M. Freer *et al.*, Phys. Rev. **C57** (1998) 1277
- [68] M. Freer *et al.*, Phys. Rev. **C51** (1995) 3174
- [69] A. Elanique, Thèse, IReS Strasbourg (1997), Report IReS 97-13
- [70] H. Chandra and U. Mosel, Nucl. Phys. **A298** (1978) 151
- [71] S.P.G. Chappell *et al.*, Phys. Lett. **444B** (1998) 260
- [72] A.H. Wuosmaa *et al.*, Phys. Rev. Lett. **68** (1992) 1295
- [73] S.P.G. Chappell *et al.*, Phys. Rev. **C51** (1995) 695
- [74] A.H. Wuosmaa *et al.*, Phys. Rev. **C54** (1996) 2463
- [75] W.D.M. Rae, A.C. Merchant, B. Buck, Phys. Rev. Lett. **69** (1992) 3709
- [76] Y. Kondo, Y. Abe and T. Matsuse, Phys. Rev. **C19** (1979) 1356
- [77] H. Flocard *et al.*, Prog. Theor. Phys. **72** (1984) 1000



- [78] T.M.. Cormier *et al.*, Phys. Rev. Lett. **40** (1978) 924, **38** (1977) 940
- [79] M. Freer *et al.*, Phys. Rev. Lett., **82** (1999) 1383
- [80] B.R. Fulton *et al.*, Phys. Lett. **B267** (1991) 325
- [81] J.S. Winfield *et al.*, J. Phys. **G25** (1999) *in press*